Vietnam Journal of Catalysis and Adsorption
Tạp chí xúc tác và hấp phụ Việt Nam

https://jca.edu.vn

Research and development of heat-resistant coating based on polyaluminium phosphate (PAP) synthesized from aluminum slag

Manh Cuong Le[1,*], Ta Lam Cuong[1]

[1] *Hanoi University of Civil Engineering, 55 Giai Phong Street, Dong Tam Ward, Hai Ba Trung District, Hanoi, Vietnam*
** Email: cuonglm@huce.edu.vn*

ARTICLE INFO

Received: 02/06/2025
Accepted: 16/06/2025
Published: 30/06/2025

Keywords:
Heat-resitant coating;
Phosphate binder;
Polyaluminium phosphate;
Aluminium Slag; Inorganic polymer

ABSTRACT

This study presents the development of a heat-resistant coating based on polyaluminium phosphate (PAP) synthesized from aluminum slag and phosphoric acid. The coating formulation included inorganic fillers such as SiO_2, TiO_2, talc, and Samot powder. The resulting coating exhibited strong adhesion (rated 5B per ASTM D3359), maintained structural integrity after exposure to temperatures up to 750 °C, and showed a total mass loss below 10% in thermogravimetric analysis (TGA). Structural and morphological analyses (SEM, XRD, EDX) confirmed the formation of stable crystalline phases including $AlPO_4$ and SiO_2. These findings support the potential application of aluminum slag-derived PAP coatings in high-temperature environments, contributing to sustainable and cost-effective material development.

Introduction

The demand for heat- and fire-resistant coatings has been steadily increasing across various industrial sectors such as construction, metallurgy, energy, and chemical processing, particularly in environments frequently exposed to flames, elevated temperatures, or corrosive conditions. While traditional organic coatings are widely used due to their ease of application, they suffer from significant limitations, including poor thermal stability, thermal decomposition, and the release of toxic fumes upon combustion [4,13]. This highlights the necessity for the development of inorganic coating systems, particularly phosphate-based coatings, as potential alternatives or complements to organic systems in high-temperature applications.

Among inorganic binders, polyaluminium phosphate (PAP) stands out due to its low-temperature curing capability, durable cross-linked network formation, excellent fire resistance, and good compatibility with various metallic substrates [1,6]. Recent studies have demonstrated that PAP can produce coatings with strong adhesion, thermal stability, and considerable insulating capacity [5,10]. However, most research to date has relied on high-purity aluminum sources such as $Al(NO_3)_3$ or $Al(OH)_3$, which are costly and energy-intensive to produce [1].

In contrast, aluminum slag a solid by-product from aluminum recycling contains significant amounts of active oxides such as Al_2O_3 and MgO, which can be used as alternative raw materials for PAP synthesis [7,11]. Utilizing aluminum slag not only reduces costs and leverages available resources but also contributes to environmental sustainability by promoting "green" materials and recycling of industrial waste [7,16]. Recent studies have also indicated that optimizing phosphate binder composition can significantly improve adhesion to metal surfaces, including chemically inert 316L stainless steel, beyond the conventional carbon steel applications [12]. Although several studies have explored the use of aluminum slag to produce refractory materials and phosphate binders [7,11], applications in

https://doi.org/10.62239/jca.2025.021

heat and fire-resistant coatings remain limited and lack comprehensive evaluations regarding structural, mechanical, and thermal performance characteristics.

Experimental and Research Methods

Materials

The chemicals and materials used in this study included: Polyaluminium phosphate (PAP) as the binder (film-forming agent) [1,3]; finely ground SiO_2 powder; TiO_2; talc; Samot powder (particle size 15–20 µm); and distilled water as the solvent.

The coating preparation procedure is as follows:

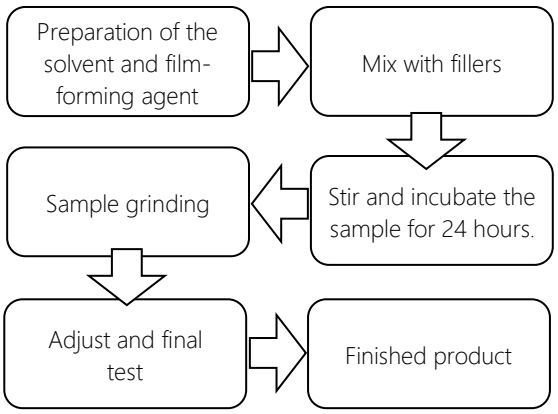

The raw materials were inspected for quality and weighed according to the following formulation: 26% PAP binder, 21% distilled water, 20% SiO_2 powder, 10% TiO_2 powder, 13% talc powder, and 10% Samot powder. According to the preparation diagram, the PAP binder was first dissolved into distilled water and stirred at a speed of 150–200 rpm. The filler powders were then gradually added into the mixture and stirred for 45 minutes at a speed of 500–600 rpm. The resulting mixture was aged for 24 hours. Subsequently, the sample was subsequently ball milling at 300–350 rpm for 75 minutes. Finally, the coating mixture was adjusted for viscosity and underwent quality evaluation before use.

Research Methods

To evaluate the thermal resistance of the coating, specimens were applied onto steel plates with dimensions of 5 × 5 cm and a thickness of 3 mm. The coated samples were left to air-dry under ambient conditions for at least 24 hours [3,4].

The direct flame heating method was carried out as follows: A handheld gas torch was used to apply direct heat to the surface of the coated samples, while an infrared thermometer was employed to monitor surface temperature during heating. Each sample was subjected to direct heating until either visible degradation occurred such as cracking, fragmentation, or delamination from the steel substrate or the target temperature was reached within 30 minutes [4].

The furnace heating method was carried out as follows: The coated samples were also subjected to incremental thermal treatment in a Nabertherm furnace (Germany) at temperatures of 400, 500, 600, 700 and 800°C. The heating rate was maintained at 10°C/min. After reaching the target temperature, the samples were held for 30 minutes, then allowed to cool gradually inside the furnace to room temperature.

The analytical methods used in this study are as follows: The microstructure and morphology of the coatings were analyzed using scanning electron microscopy (SEM), X-ray diffraction (XRD), thermogravimetric analysis (TGA), and energy-dispersive X-ray spectroscopy (EDX).

Results and Discussion

Physical and Mechanical Properties of the Coating:

The physical and mechanical properties of the coating are presented in Table 1.

Table 1. Physical and mechanical properties of the coating

Property	Value
Flexural strength ($N.mm^2$)	5.0 ± 0.2
Adhesion (MPa)	0.40 ± 0.03
Hardness	HB
Impact resistance (N)	8.0 ± 0.5
Viscosity (mPa·s)	489 ± 12
Fineness (µm)	20 ± 1

The adhesion is quite good for inorganic coatings, meeting the ASTM D3359 standard at 5B (no peeling), which reflects the strong bond with the steel substrate of PAP [1,6]. HB hardness is average, with the ability to resist light scratches. Impact resistance is average compared to other inorganic coatings [7]. Bending strength is average. The coating structure exhibits a certain hardness without being too brittle, which helps the coating resist cracking due to stress or light mechanical impact [5,7]. High viscosity and low smoothness are the advantages of the coating, increasing the ability to cover, not being rough and scratched during the drying process.

Regarding the heat resistance results of the coating layer: The coating samples on steel substrates were heated at different and increasing temperatures: 25 –

https://doi.org/10.62239/jca.2025.021

800°C using a Nabertherm (Germany) heating device with a heating rate of 10°C/min. After reaching the required heating temperature, the samples were kept in the furnace for 30 minutes, then slowly cooled in the furnace to room temperature. The research results showed that the coating samples were able to withstand heat up to 750°C and maintain adhesion on the steel substrate. This is a highlight compared to traditional inorganic paint systems that often lose their physical and mechanical properties when exposed to high temperatures [3,5].

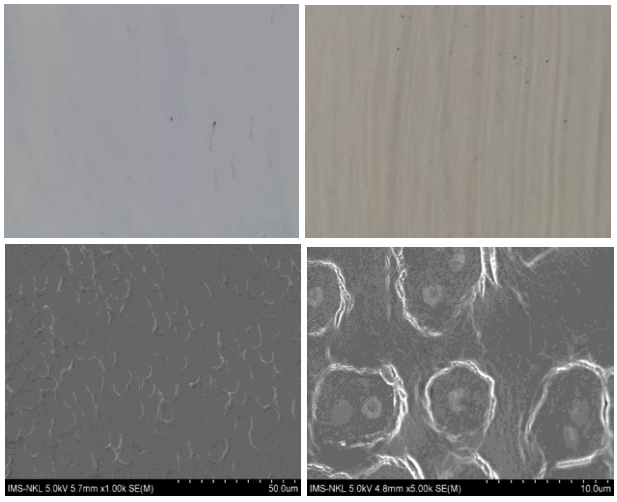

Figure 1. Coating samples before (a) and after (b) calcination at 800 °C.

Figure 2 illustrates the surface thermal shock resistance of the coating subjected to direct flame torch testing.

Figure 2. Coating after direct flame thermal shock test

After thermal shock, torching of the coating sample was performed by focusing on a point in the middle of the sample. The front surface of the coated sample was still solid, with no signs of peeling, and the color was slightly dark brown. Compared with studies using pure aluminum sources such as $Al(NO_3)_3$ or $Al(OH)_3$ [1], the use of aluminum slag not only helps to utilize industrial waste but also achieves equivalent or even superior properties thanks to the presence of active phases such as Al_2O_3 and MgO in the slag [7,16,19]. This is also consistent with the orientation of developing sustainable and environmentally friendly materials in the field of refractory materials. Additionally, thermal shock tests showed that the coating did not peel or crack noticeably after being directly torched at over 700°C, Recent developments in phosphate-based coatings for cultural heritage protection have highlighted their dual role in both thermal shielding and preservation of underlying materials [8]. Such coatings, when optimized with industrial by-products, exhibit enhanced compatibility with aged substrates and demonstrate reduced micro-cracking during thermal cycling, making them suitable not only for industrial but also for architectural applications.

Indicating good resistance to instantaneous thermal stress, as an important factor in industrial applications such as protective coatings for furnaces, hot air ducts, or metal surfaces exposed to direct fire [5,9,10].

Figure 3 presents the thermogravimetric analysis (TGA) results of the coating.

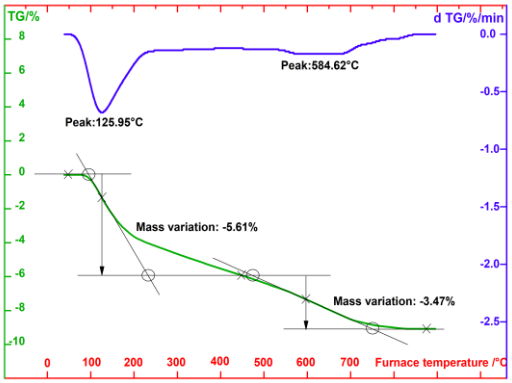

Figure 3. TGA curve of the coating.

The results showed that the coating sample was heat-resistant at nearly 600°C. Based on the TGA spectrum, the stages of the sample were:

Stage 1 (30 – 200°C): 5.61% mass loss, with a peak at 125.95°C. This is the process of evaporation of free water and chemically bound water in the polyphosphate system. This stage is common with inorganic binder systems of phosphate or silicate origin [1,6].

Stage 2 (450 – 750°C): 3.47% loss, with a peak at 584.62°C. This stage is related to the gradual decomposition of the polyaluminium phosphate network, and at the same time, the decomposition reaction of some residual aluminum and magnesium oxide from the slag may occur [7,13].

https://doi.org/10.62239/jca.2025.021

The total mass loss of less than 10% over the entire temperature range investigated shows that the coating has very high thermal stability, especially when compared to organic or epoxy paint systems (which often decompose strongly at 300–500°C) [4,6,15]. In addition, the TGA spectrum does not show any abrupt decomposition regions, indicating that the coating structure does not contain volatile organic compounds or unstable components. This is a great advantage in fire-resistant, flame-retardant coating applications or working in harsh environments [5,13,18]. Polymeric reinforcement strategies using inorganic–organic hybrids have shown significant improvements in thermal shock resistance and film flexibility [17]. Particularly, incorporation of phosphates into polymer matrices allows tailoring of mechanical properties while maintaining fire-retardant performance a key advantage for high-temperature coatings requiring both structural resilience and environmental safety.

Figure 4 presents the X-ray diffraction (XRD) analysis results of the coating.

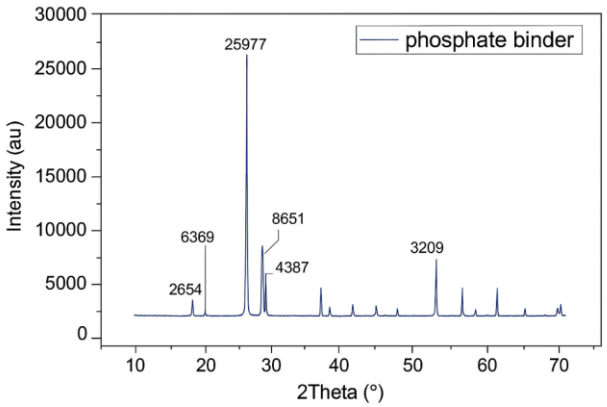

Figure 4. XRD pattern of the coating

X-ray diffraction (XRD) analysis was performed to identify the crystalline phases formed in the coating after curing and calcination at high temperatures. The XRD spectra presented in Figure 4 show the presence of several characteristic crystalline phases:

• 2θ angle ≈ 18.5–21.0°: Diffraction peaks corresponding to the $AlPO_4$ phase, which is a product formed from the reaction between Al^{3+} ions from aluminum slag and PO_4^{3-} groups during the synthesis of the binder, appear. The presence of $AlPO_4$ proves the formation of a stable and heat-resistant inorganic bonding network [1,6,16].

• 2θ angle ≈ 26.6°: A strong peak of SiO_2 (quartz) is recorded, which acts as the main filler and simultaneously creates a ceramic framework that supports geometric stability and improves heat resistance [2,5].

• 2θ angle ≈ 29.1–32.0°: Diffraction peaks of MgO and TiO_2 phases were recorded, which may come from impurities in aluminum slag and titanium pigments used in the paint system. The presence of these metal oxides contributes to improving the thermal stability and mechanical strength of the coating [5,13].

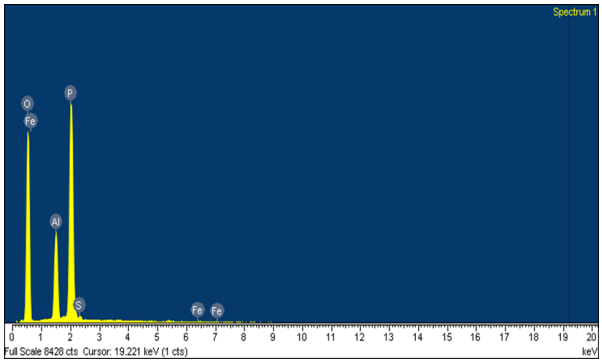

Figure 5. EDX spectrum of the cured coating surface

Energy dispersive X-ray spectroscopy (EDX) analysis was performed to determine the elemental composition of the cured coating surface. The EDX results showed that the coating contained the following main elements:
O (oxygen), P (phosphorus), Al (aluminum): These are the three main elements, directly related to the polyphosphate network structure of the PAP adhesive. The clear presence of P and Al confirms the effectiveness of the adhesive synthesis from aluminum slag and phosphoric acid [1,6,16].

Si (silicon): Derived from quartz powder (SiO_2) in the filler composition, plays a role in enhancing the heat resistance and impact resistance of the coating [5,2].
Ti (titanium): Present in significant amounts from TiO_2 powder, plays a role as a colorant and increases the ability to reflect heat [5,13].

Fe, Cr, Zn: May be impurities from the steel substrate or residual due to incomplete surface treatment. However, these elements do not significantly affect the properties of the coating [14].

Conclusion

This study successfully developed a heat-resistant coating based on PAP synthesized from aluminum slag. The coating exhibited strong adhesion (5B) and high thermal resistance up to 750 °C. SEM analysis revealed a dense and uniform coating surface, while XRD confirmed the formation of crystalline $AlPO_4$, SiO_2, and MgO/TiO_2 phases that contributed to thermal and mechanical stability. TGA results indicated a total mass loss below 10%, reflecting excellent thermal degradation resistance. These structural insights explain the coating's

https://doi.org/10.62239/jca.2025.021

ability to maintain integrity under high heat and thermal shock. The use of aluminum slag not only reduces raw material cost but also supports sustainable, environmentally friendly coating development for high-temperature industrial applications.

Beyond technical performance, the use of aluminum slag as a raw material contributes significantly to environmental sustainability. It reduces reliance on high-purity aluminum compounds, minimizes landfill waste, and supports circular economy principles in materials engineering. By valorizing industrial by-products, this approach also lowers the environmental footprint of the coating production process.

References

1. Y. Li, G. Chen, S. Zhu, H. Li, Z. Ma, Y. B. Liu, L. Liu, Bull. Mater. Sci. 42 (2019) 200. https://doi.org/10.1007/s12034-019-1912-3
2. B. Zhang, W. Gong, X. Li, P. Chen, B. Zhu, Mater. Res. 110 (2019) 765–772. https://doi.org/10.3139/146.111796
3. C. M. Le, T.-H. Le, J. Anal. Methods Chem. (2021) Article ID 5510193. https://doi.org/10.1155/2021/5510193
4. T. V. La, Chemistry Journal 48 (4A) (2010) 485–488
5. G. Cai, J. Wu, J. Guo, Y. Wan, Q. Zhou, P. Zhang, X. Yu, M. Wang, Materials 16 (13) (2023) 4498. https://doi.org/10.3390/ma16134498
6. D. D. L. Chung, Mater. Sci. Lett. 38 (2003) 2785–2791. https://doi.org/10.1023/A:1024446014334
7. A. Mikhailova et al., Procedia Eng. 206 (2017) 1376–1381. https://doi.org/10.1016/j.proeng.2017.10.698
8. Ines Soares, Joana Lia Ferreira, Helena Silva, Maria Paula Rodrigues, Journal of Cultural Heritage 66 (2024) 208–218. https://doi.org/10.1016/j.culher.2024.06.014
9. B. Zhang et al., Surf. Coat. Technol. 460 (2023) 128524. https://doi.org/10.1016/j.surfcoat.2023.128524
10. H. Wei, T. Wang, Q. Zhang, Y. Jiang, C. Mo, J. Chin. Chem. Soc. 67 (2020) 116–124. https://doi.org/10.1002/jccs.201900008
11. D. Chen, L. He, S. Shang, Mater. Sci. Eng. A 348 (2003) 29–35. https://doi.org/10.1016/S0921-5093(02)00643-3
12. S. Huo, Z. Dong, X. Li, P. Liu, P. Chen, B. Zhu, Int. J. Adhes. 125 (2023). https://doi.org/10.1016/j.ijadhadh.2023.103437
13. M. Wang, Z. Liang, S. Yan, X. Tao, Y. Zou, J. Li, X. Zhou, H. Zhang, Constr. Build. Mater. 359 (2022). https://doi.org/10.1016/j.conbuildmat.2022.129480
14. M. Vippola, S. Ahmaniemi, J. Keränen, P. Vuoristo, T. Lepistö, T. Mäntylä, E. Olsson, Mater. Sci. Eng. A 323 (2002) 1–8. https://doi.org/10.1016/S0921-5093(01)01367-3
15. S. N. Chen, C. Lin, H. L. Hsu, X. H. Chen, Y. C. Huang, T. H. Hsieh, K. S. Ho, Y. J. Lin, Materials 15 (2022). https://doi.org/10.3390/ma15155317
16. M. Vippola, J. Keränen, X. Zou, S. Hovmöller, T. Lepistö, T. Mäntylä, J. Am. Ceram. Soc. 83 (2000) 1834–1836. https://doi.org/10.1111/j.1151-2916.2000.tb01477.x
17. Eldipa Piperopoulos, Giuseppe Scionnti, Mario Atria, Luigi Calabrese, Edoardo Proverbio, Polymers 14(3) (2022) 372. http://dx.doi.org/10.3390/polym14030372
18. J. Li, J. Liu, Y. Zhang, Y. Wan, J. Liu, G. Cai, X. Tao, W. Jing, M. Wang, Ceram. Int. (2024). https://doi.org/10.1016/j.ceramint.2024.08.440
19. C. Qi, X. Ji, J. Li, Z. Hu, X. Wei, B. Xiao, M. Wang, J. Eur. Ceram. Soc. 45 (2025). https://doi.org/10.1016/j.jeurceramsoc.2025.117356